Cancer Management and Research

Dovepress

open access to scientific and medical research

Open Access Full Text Article

ORIGINAL RESEARCH

Long Noncoding RNA PRR34-AS1 Aggravates the Progression of Hepatocellular Carcinoma by Adsorbing microRNA-498 and Thereby Upregulating FOXO3

This article was published in the following Dove Press journal:
Cancer Management and Research

Zhaoming Liu[1]
Zhen Li[2]
Binghui Xu[1]
Hao Yao[1]
Shuangyu Qi[1]
Jianxiong Tai[1]

[1]Department of Hepatobiliary Surgery, Harrison International Peace Hospital, Hengshui, Hebei 053000, People's Republic of China; [2]Department of Interventional Therapy, Harrison International Peace Hospital, Hengshui, Hebei 053000, People's Republic of China

Purpose: Long noncoding RNAs are differentially expressed in hepatocellular carcinoma (HCC) and have been validated as essential regulators in HCC. However, there is limited knowledge regarding the detailed roles and mechanisms of most lncRNAs in HCC cells. In this study, the expression profiles of PRR34 antisense RNA 1 (*PRR34-AS1*) in HCC tissues and cell lines were determined. In addition, the detailed roles and underlying mechanisms of PRR34-AS1 in HCC cells were comprehensively elucidated.

Methods: Reverse transcription-quantitative polymerase chain reaction (PCR) was performed to measure *PRR34-AS1* expression in HCC cells. Cell proliferation, apoptosis, and migration and invasion were evaluated in vitro using the cell counting kit-8 (CCK-8) assay, flow cytometric analysis and transwell cell migration and invasion assays, respectively. In vivo tumor growth was determined using tumor xenograft experiments. The potential miRNA targets of *PRR34-AS1* were predicted via bioinformatic analysis and further confirmed using the luciferase reporter assay, RNA immunoprecipitation assay, and reverse transcription-quantitative PCR.

Results: *PRR34-AS1* was highly expressed in HCC tissues and cell lines, and its interference suppressed HCC cell proliferation, migration, and invasion but promoted cell apoptosis in vitro. In addition, loss of *PRR34-AS1* decreased tumor growth in HCC cells in vivo. Mechanistically, PRR34-AS1 functions as a *miR-498* sponge and subsequently increases forkhead box O3 (*FOXO3*) expression in HCC cells. Rescue experiments revealed that the suppressive effects triggered by *PRR34-AS1* knockdown on the malignant characteristics of HCC cells could be abrogated by inhibiting *miR-498* or restoring *FOXO3* expression.

Conclusion: The depletion of *PRR34-AS1* suppresses the oncogenicity of HCC cells by targeting the miR-498/FOXO3 axis. Therefore, the PRR34-AS1/miR-498/FOXO3 pathway may offer a basis for HCC treatment.

Keywords: PRR34 antisense RNA 1, forkhead box O3, ceRNA regulation model, polymerase chain reaction

Introduction

Hepatocellular carcinoma (HCC) is the fifth-most common type of human cancer and the second-most common cause of cancer-related mortalities worldwide[1] due to a lack of noticeable symptoms, difficulties in early detection, complex pathological mechanisms, and high death rates.[2] In the last decade, the morbidity of HCC has

Correspondence: Zhaoming Liu
Department of Hepatobiliary Surgery, Harrison International Peace Hospital, 180 Renmin East Road, Hengshui, Hebei 053000, People's Republic of China
Email liuzm_hepat@163.com

submit your manuscript | www.dovepress.com
DovePress
http://doi.org/10.2147/CMAR.S263619

significantly increased by approximately 3% per year in women and by approximately 4% per year in men.[3] It has been estimated that there will be over 750,000 novel HCC cases and 55,000–85,000 deaths per year globally due to this fatal malignancy.[4] Despite tremendous advancements in HCC diagnosis and therapy, the therapeutic effectiveness of HCC treatments remains unsatisfactory, with more than half of the patients suffering from recurrence and distant metastasis even after surgical excision.[5,6] The overall 5-year survival rate of patients with HCC is approximately 5%, and the poor clinical outcomes are largely attributed to limited effective treatment options, delayed diagnosis, and the complex pathogenesis of HCC.[7,8] Therefore, research into the mechanisms associated with hepatocarcinogenesis and cancer progression may contribute in identifying promising therapeutic targets as well as in developing new approaches for HCC management.

Long noncoding RNAs (lncRNAs) are short transcripts (over 200 nucleotides long) that lack protein-coding capacity.[9] Several studies have revealed that lncRNAs contribute to diverse physiological and pathological processes via epigenetic, transcriptional, and post-transcriptional modulation.[10] Accumulating evidence suggests that lncRNAs play key roles in carcinogenesis and cancer progression.[11–13] The aberrant expression of lncRNAs is commonly observed in HCC cells. For instance, SNHG5,[14] OIP5-AS1,[15] and CASC[16] are upregulated in HCC cells, whereas RMRP,[17] AND2-AS1[18] and MIR22HG[19] are expressed at low levels. The dysregulation of lncRNAs can have oncogenic or anti-oncogenic effects, and lncRNAs function in the regulation of numerous malignant characteristics.[20,21]

MicroRNAs (miRNAs) are a subgroup of noncoding RNA molecules of approximately 17–24 nucleotides. They can negatively regulate gene expression by base pairing with the 3′-untranslated regions (3′-UTRs) of their target mRNAs, resulting in transcript inhibition and/or mRNA degradation.[22] To date, 474 miRNAs have been verified in the human genome and are estimated to regulate approximately 30% of protein-coding genes.[23] They are critically implicated in the genesis and development of HCC because they exert essential activities, such as the regulation of cell growth, metastasis, tumor differentiation, and angiogenesis.[24,25] Importantly, the proposed competing endogenous RNA (ceRNA) theory, which suggests that lncRNAs work as a miRNA sponge and prevent their binding to mRNAs, has received increasing attention.[26] Therefore, it may be helpful to study the functions and mechanisms of lncRNAs in HCC cells to identify effective therapeutic targets.

A substantial number of lncRNAs are aberrantly expressed in HCC;[27,28] however, knowledge regarding the detailed roles and mechanisms of most lncRNAs in HCC cells remains limited. In this study, we first measured PRR34 antisense RNA 1 (PRR34-AS1) expression in HCC cells and tissues and determined the roles of PRR34-AS1 in regulating the malignant characteristics of HCC cells. In addition, we comprehensively elucidated the mechanisms behind the oncogenic functions of PRR34-AS1 in HCC cells.

Materials and Methods

Tissue Sample and Cell Culture

HCC and adjacent normal tissues were collected from 65 patients in Harrison International Peace Hospital. All enrolled patients had not received radiotherapy, chemotherapy, or other anticancer treatments before the operation. All tissue specimens were immediately placed into liquid nitrogen and stored in liquid nitrogen until further use. This study was approved by the Ethics Committee of Harrison International Peace Hospital (2020#063) and performed in accordance with the Declaration of Helsinki. Written informed consent was obtained from all participants.

HCC cell lines, including Hep3B, HuH7, and BEL-7402, as well as transformed Human Liver Epithelial-3 cells (THLE-3) were purchased from the Cell Bank of the Chinese Academy of Sciences (Shanghai, China). Two additional HCC cell lines (SNU-182 and SNU-398) were obtained from American Type Culture Collection (Manassas, VA, USA).

Hep3B cells were maintained in minimal essential medium (Gibco; Thermo Fisher Scientific, Inc., Waltham, MA, USA) containing 10% fetal bovine serum (FBS; Gibco; Thermo Fisher Scientific, Inc.), 1% GlutaMAX, 1% nonessential amino acids, 1% sodium pyruvate 100 mM solution, and 1% penicillin/streptomycin (Gibco; Thermo Fisher Scientific, Inc.). HuH7 cells were cultured in Dulbecco's Modified Eagle Medium (Gibco; Thermo Fisher Scientific, Inc.) with 10% FBS, 1% GlutaMAX, 1% nonessential amino acids, and 1% penicillin/streptomycin. RPMI-1640 (Gibco; Thermo Fisher Scientific, Inc.) containing 10% heat-inactivated FBS (Gibco; Thermo Fisher Scientific, Inc.) and 1% penicillin/streptomycin was used for the culturing of BEL-7402, SNU-182, and SNU-398

cells. Extra 1% GlutaMAX and 1% nonessential amino acids were added to the growth medium for SNU-182 cells. BEGM medium (Clonetics Corporation, Walkersville, MD) with 5 ng/mL EGF, 70 ng/mL Phosphoethanolamine and 10% FBS was used to culture THLE-3 cells. All cell lines were cultured at 37°C in a humidified atmosphere of 5% CO_2.

Oligonucleotide, Plasmid, and Cell Transfection

miR-498 mimic and inhibitor were obtained from Ribobio (Guangzhou, China) and used to increase and decrease endogenous *miR-498* expression, respectively. Negative control miRNA mimic (miR-NC) and negative control (NC) inhibitor were used as the controls for miR-498 mimic and miR-498 inhibitor, respectively. The corresponding sequences were as follows: miR-498 mimic, 5′-CUUUUUGCGGGGGACCGAACUUU-3′; miR-NC, 5′-UUGUACUACACAAAAGUACUG-3′; miR-498 inhibitor, 5′- GAAAAACGCCCCCUGGCUUGAAA −3′; and NC inhibitor 5′-CAGUACUUUUGUGUAGUACAA-3′.

Small interfering RNA (siRNA) targeting *PRR34-AS1* (si-PRR34-AS1), siRNA scrambled control (si-NC), the forkhead box O3 (*FOXO3*) overexpressing plasmid pcDNA3.1/FOXO3, and empty pcDNA3.1 plasmid were all acquired from GenePharma Co., Ltd, (Shanghai, China). These oligonucleotides and plasmids were transfected into HCC cells using the Lipofectamine 2000 reagent (Invitrogen, Carlsbad, CA, USA). The si-PRR34-AS1 sequences were as follows: si-PRR34-AS1#1, 5′-UCAAUAATGCAAAAAA ATTTA-3′; si-PRR34-AS1#2, 5′-AUUTATTTGACTTATA ATAAATA-3′; and si-PRR34-AS1#3, 5′-UCGTTTTGTTT TGATTTATTTTA-3′. The si-NC sequence was 5′-CACGAT AAGACAATGTAT-3′.

Cellular Nucleocytoplasmic Fractionation

Nuclear and cytoplasmic fractions were isolated using the Cytoplasmic and Nuclear RNA Purification Kit (Norgen Biotek, Thorold, Canada). The abundance of *PRR34-AS1* in the nuclear and cytoplasmic fractions was evaluated via reverse transcription-quantitative polymerase chain reaction (RT-qPCR).

RT-qPCR

Total RNA was extracted from the cells using the TRIzol reagent (Invitrogen; Thermo Fisher Scientific, Inc.). The miRcute miRNA Isolation Kit (TIANGEN, Beijing, China) was used for miRNA extraction. RNA purity and quality were determined using the NanoDrop 2000c (Thermo Fisher Scientific, Inc.). Complementary DNA (cDNA) was synthesized from total RNA using the PrimeScript™ RT Reagent Kit (Takara Biotechnology Co., Ltd., Dalian, China), and qPCR was performed to detect the expression of *PRR34-AS1* and *FOXO3* using the SYBR® Premix Ex Taq™ (Takara Biotechnology Co., Ltd.). Glycerol-3-phosphate dehydrogenase (*GAPDH*) was used as the internal reference for *PRR34-AS1* and *FOXO3* expression.

The miRcute Plus miRNA First-Strand cDNA Kit (TIANGEN) was used to synthesize cDNA from miRNA. The cDNA was then subjected to PCR amplification to measure miR-498 expression using the miRcute Plus miRNA qPCR Kit (TIANGEN). The expression of *miR-498* was normalized to that of *U6* small nuclear RNA. Gene expression was analyzed using the 2−ΔΔCt method.

The primers were designed as follows: PRR34-AS1, 5′-CGATTTGGCCTTAACTTATTGA-3′ (forward) and 5′-ATGCTTACAGAAGATAATCAACAGGTA −3′ (reverse); FOXO3, 5′-ACTCATGCAGCGGAGCTCTAG-3′ (forward) and 5′-GTTCAGAGATGAAGGTCCGAACA-3′ (reverse); GAPDH, 5′-CGGAGTCAACGGATTTGGTC GTA (forward) and 5′-AGCCTTCTCCATGGTGGTG AAGAC-3′ (reverse); miR-498, 5′- TCGGCAGGUUCA AGCCAGGGG −3′ (forward) and 5′- CACTCAACTG GTGTCGTGGA −3′ (reverse); and U6, 5′-GCTTCGGCA GCACATATACTAAAAT-3′ (forward) and 5′-CGCTTCA CGAATTTGCGTGTCAT-3′ (reverse).

Cell Counting Kit-8 (CCK-8) Assay

Transfected cells were seeded into 96-well plates with five replicate wells. Each well contained a 100-µL cell suspension containing 2000 cells. Cell proliferation was monitored at 0, 24, 48, and 72 h after cell inoculation. Cells were incubated with 10 µL of the CCK-8 solution (Dojindo, Tokyo, Japan) at 37°C with 5% CO_2 for 2 h. Finally, the absorbance was measured at 450 nm using a microplate reader.

Flow Cytometric Analysis

Transfected cells were detached by incubating them with ethylenediaminetetraacetic acid (EDTA)-free 0.25% trypsin and then rinsing them twice with ice-cooled phosphate buffer solution. Following centrifugation, the apoptosis of the transfected cells was detected using the Annexin V-fluorescein isothiocyanate (FITC) Apoptosis Detection Kit (Biolegend, San Diego, CA, USA). Briefly, transfected cells collected in a flow cytometer tube were made into

a cell suspension and subsequently stained with 10 μL of annexin V-FITC and 5 μL of propidium iodide at room temperature for 20 min in the dark. The ratio of apoptotic cells was analyzed using a flow cytometer (FACScan; BD Biosciences, Franklin Lakes, NJ, USA).

Transwell Cell Migration and Invasion Assays

For cell migration, transfected cells were collected after 48 h of cultivation and suspended in FBS-free basal medium at a density of 5×10^5 cells/mL. The upper compartments of the transwell chambers (8-μm pore size; Corning Glass Works, Corning, N.Y., USA) were filled with 200 μL of the cell suspension, whereas 500 μL of the culture medium supplemented with 20% FBS were added into the basolateral compartments. After 24 h, the nonmigrated cells were removed with a cotton swab and the migrated cells were treated with 100% methanol and stained with 0.5% crystal violet. For cell invasion, the transwell chambers were coated with Matrigel (BD Biosciences, Franklin Lakes, NJ, USA), and the remaining procedures were similar to those of the migration assay. The migrated and invaded cells were imaged and counted using an IX31 inverted microscope (x200 magnification; Olympus Corporation, Tokyo, Japan).

Tumor Xenograft Experiment

The lentiviral vectors expressing short hairpin RNA (shRNA) sequences targeting *PRR34-AS1* (sh-PRR34-AS1) and shRNA scrambled control (sh-NC) were prepared by GenePharma Co., Ltd. HuH7 cells were infected with the lentiviral vectors and incubated with puromycin to select the sh-PRR34-AS1 stably silenced HuH7 cells. The sequences of sh-PRR34-AS1 were 5′-CCGGCTC TAATAATGGXAAAXAATTXCTCGAGTAAATTTTT-TTCCATTXTAGAXTTTTTG-3′ and the sh-NC sequences were 5′-CCGGCACGATAAGACAATGTATT TCTCGAGAAAXCATTGTCTTATCGTGTTTTTG-3′.

Male BALB/c nude mice (aged 4–6 weeks) were purchased from the Shanghai experimental animal center at the Chinese academy of sciences (Shanghai, China) and were randomly assigned into two groups: sh-PRR34-AS1 and sh-NC groups. The mice in the sh-PRR34-AS1 group were subcutaneously injected with approximately 1×10^7 HuH7 cells stably expressing sh-PRR34-AS1, whereas mice in the sh-NC group were inoculated with sh-NC stably transfected cells. After 1 week, tumor size was monitored every 4 days. All mice were euthanized at the end of the 31th day. Tumor xenografts were harvested, weighed, and preserved in liquid nitrogen. Tumor volume was calculated using the following formula: volume = 0.5 × (length × width^2). All animal protocols were approved by the Institutional Animal Care and Use Committee of Harrison International Peace Hospital (2018#105), and performed in accordance with the NIH guidelines for the care and use of laboratory animals.

Bioinformatic Analysis

The expression profile of *PRR34-AS1* in HCC cells and tissues and its relationship with overall survival were analyzed using the Gene Expression Profiling Interactive Analysis (GEPIA; http://gepia.cancer-pku.cn/), which includes the TCGA and GTEx databases. The potential miRNA targets of *PRR34-AS1* were predicted using StarBase version 3.0 (http://starbase.sysu.edu.cn/). lncLocator (http://www.csbio.sjtu.edu.cn/bioinf/lncLocator) a lncRNA subcellular localization predictor, was used to predict the location of *PRR34-AS1*.

RNA Immunoprecipitation (RIP) Assay

The EZ-Magna RIP™ RNA-Binding Protein Immunoprecipitation Kit (Millipore, Billerica, MA, USA) was used to perform the RIP assay. HCC cells were collected and incubated with RIP lysis buffer. The cell lysates were incubated overnight at 4°C with magnetic beads conjugated with anti-argonaute 2 (Ago2) or control IgG antibody (Millipore). After digestion with protease K, the immunoprecipitated RNA was extracted and subjected to RT-qPCR analysis to determine *miR-498* and *PRR34-AS1* enrichment.

Luciferase Reporter Assay

The fragments of *PRR34-AS1* containing the *miR-498* wild-type (wt) binding site was amplified using RT-qPCR and then inserted into pmirGLO dual-luciferase reporter vectors (Promega, Madison, WI, USA), generating the wt-PRR34-AS1 reporter plasmid. The GeneTailor™ Site-Directed Mutagenesis System (Invitrogen, Carlsbad, CA, USA) was used to perform binding site-directed mutagenesis and to produce the PRR34-AS1 mutant (mut) reporter plasmid mut-PRR34-AS1. The wt-FOXO3 and mut-FOXO3 reporter plasmids were constructed following the same experimental steps. Using the Lipofectamine 2000 reagent, wt or mut reporter plasmids alongside miR-498 mimic or miR-NC were introduced into HCC cells. After

48 h, the luciferase activity was determined using the Dual-Luciferase Assay Kit (Promega).

Western Blotting

Total protein was extracted from cultured cells using RIPA Lysis and Extraction Buffer (Invitrogen, Carlsbad, CA, USA). The concentration of total protein was detected using the BCA Protein Assay Kit (Beyotime; Shanghai, China). Equal amounts of protein were separated using 10% sodium dodecyl sulfate–polyacrylamide gel electrophoresis and transferred onto polyvinylidene fluoride membranes. After blocking with 5% skimmed milk for 2 h, the membranes were incubated overnight with specific primary antibodies targeting FOXO3 (cat. No. ab109629; Abcam, Cambridge, UK) or GAPDH (cat. No. ab181603; Abcam) and then probed with a horseradish peroxidase-conjugated goat anti-rabbit immunoglobulin G secondary antibody (cat. No. ab205718; Abcam). Finally, the Enhanced Chemiluminescence Detection System (Pierce; Thermo Fisher Scientific, Inc.) was used to develop protein signals.

Statistical Analysis

All results from three biological replicates were presented as mean ± standard deviation. The Student's *t*-test was used to compare the data between the two groups, whereas the one-way analysis of variance followed by Tukey's test was performed to test the difference among multiple groups. The chi-square test was used to determine the association between *PRR34-AS1* expression and clinicopathological parameters in 65 HCC patients. The expression correlation between the two genes in the HCC tissues was determined using Pearson's correlation coefficient. The overall survival rate was analyzed using the Kaplan–Meier method and evaluated with the Log rank test. $P < 0.05$ was considered to indicate statistical significance.

Results

PRR34-AS1 is Upregulated in HCC Cells, and Its Depletion Suppresses Cancer Progression

To determine the expression of *PRR34-AS1* in HCC cells, GEPIA was used to analyze *PRR34-AS1* expression in the TCGA and GTEx databases. The expression of *PRR34-AS1* was upregulated in HCC tissues than in normal tissues (Figure 1A). To validate this observation, RT-qPCR was performed to detect *PRR34-AS1* expression in 65 pairs of HCC and adjacent normal tissues. The data revealed that *PRR34-AS1* was remarkably upregulated in HCC tissues than in adjacent normal tissues (Figure 1B). Additionally, the expression levels of *PRR34-AS1* were measured in HCC cell lines (Hep3B, HuH7, BEL-7402, SNU-182, and SNU-398) and transformed Human Liver Epithelial-3 (THLE-3). Consistently, the expression level of *PRR34-AS1* was higher in all five HCC cell lines than in THLE-3 (Figure 1C). Furthermore, data analysis obtained from TCGA and GTEx revealed that there was no obvious correlation between *PRR34-AS1* expression and overall survival in patients with HCC (Figure 1D; P = 0.14), which is consistent with the results obtained from the Kaplan–Meier analyses of the 65 HCC patients (Figure 1E; P = 0.178).

Among the five HCC cell lines examined, HuH7 and SNU-182 relatively exhibited the highest *PRR34-AS1* expression and were therefore selected for further experiments. *PRR34-AS1* expression was silenced in HuH7 and SNU-182 cells with the transfection of si-PRR34-AS1. The silencing efficiency was verified using RT-qPCR. The results demonstrated the decreased expression of *PRR34-AS1* in HuH7 and SNU-182 cells after the introduction of si-PRR34-AS1 (Figure 1F). si-PRR34-AS1#1 exhibited the highest efficiency in knocking down *PRR34-AS1* expression and was therefore used in subsequent functional experiments. The CCK-8 assay and flow cytometric analysis were performed to assess HCC cell proliferation and apoptosis after *PRR34-AS1* knockdown. We observed that loss of *PRR34-AS1* clearly hindered the proliferation (Figure 1G) but induced the apoptosis (Figure 1H) of HuH7 and SNU-182 cells. Furthermore, both migratory (Figure 1I) and invasive (Figure 1J) abilities were apparently decreased in PRR34-AS1-silenced HuH7 and SNU-182 cells, as evidenced by the transwell cell migration and invasion assay results. Taken together, these findings suggest that *PRR34-AS1* is upregulated in HCC cells and that it exhibits an oncogenic regulatory role in HCC malignancies.

PRR34-AS1 Functions by Adsorbing miR-498 in HCC Cells

To explore the detailed mechanisms by which *PRR34-AS1* regulates the oncogenicity of HCC, lncLocator analysis and cellular nucleocytoplasmic fractionation were performed to determine its localization in HCC cells. *PRR34-AS1* was predicted to be located in the cytoplasm (Figure 2A).This prediction was reconfirmed using the cellular

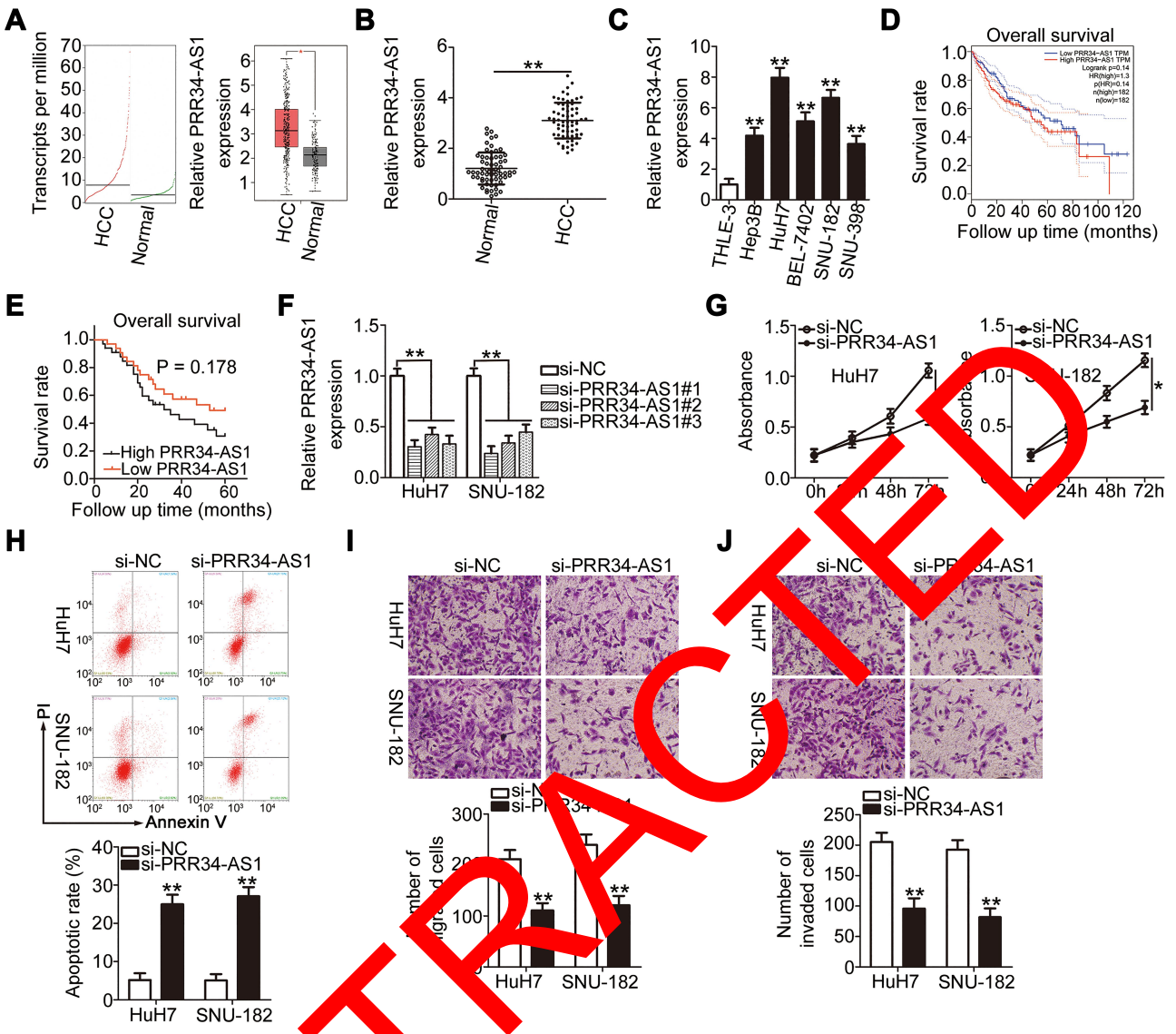

Figure 1 Knockdown of *PRR34-AS1* inhibits HCC progression. (**A**) *PRR34-AS1* expression in HCC and normal liver tissues from the TCGA and GTEx databases. (**B**) RT-qPCR detection of the expression of *PRR34-AS1* in 65 pairs of HCC and adjacent normal tissues. (**C**) RT-qPCR analysis was used to determine *PRR34-AS1* expression in HCC cell lines (Hep3B, HuH7, BEL-7402, SNU-182, and SNU-398) and transformed Human Liver Epithelial-3 (THLE-3). (**D**) TCGA and GTEx databases were used to analyze the overall survival rates of patients with HCC with high or low **PRR34-AS1** expression. (**E**) Kaplan–Meier analysis was conducted to determine the correlation between *PRR34-AS1* expression and the overall survival rate of patients with HCC. (**F**) HuH7 and SNU-182 cells were transfected with si-PRR34-AS1 or si-NC. The knockdown efficiency of si-PRR34-AS1 was assessed via RT-qPCR. (**G** and **H**) CCK-8 assays and flow cytometric analysis were used to detect the proliferation and apoptosis of HuH7 and SNU-182 cells after *PRR34-AS1* depletion, respectively. (**I** and **J**) Transwell cell migration and invasion assays were used to determine the effects of *PRR34-AS1* silencing on the migratory and invasive capabilities of HuH7 and SNU-182 cells (x200 magnification). *P < 0.05 and **P < 0.01.

nucleocytoplasmic fractionation assay (Figure 2B). Extensive evidence has shown that cytoplasmic lncRNAs can act as miRNA sponges, functionally liberating miRNA-targeted mRNAs. Bioinformatic analysis was conducted to identify potential miRNAs with complementary base pairing to PRR34-AS1. Two miRNAs, *miR-498* and *miR-3614-5p*, were predicted to be sequestered by *PRR34-AS1* (Figure 2C). After *PRR34-AS1* knockdown in HuH7 and SNU-182 cells, the expression levels of miR-498 were found to be increased, whereas those of *miR-3614-5p* were unaffected (Figure 2D). Therefore, *miR-498* was selected for further experiments.

miR-498 expression was detected in the 65 pairs of HCC and adjacent normal tissues. RT-qPCR analysis showed that *miR-498* was evidently downregulated in HCC tissues than in adjacent normal tissues (Figure 2E). Furthermore, the expressions of *PRR34-AS1* and *miR-498* were inversely correlated in the 65 HCC tissues (Figure 2F; $r = -0.7021$, $P < 0.0001$), as demonstrated using Pearson's correlation coefficient. Luciferase reporter

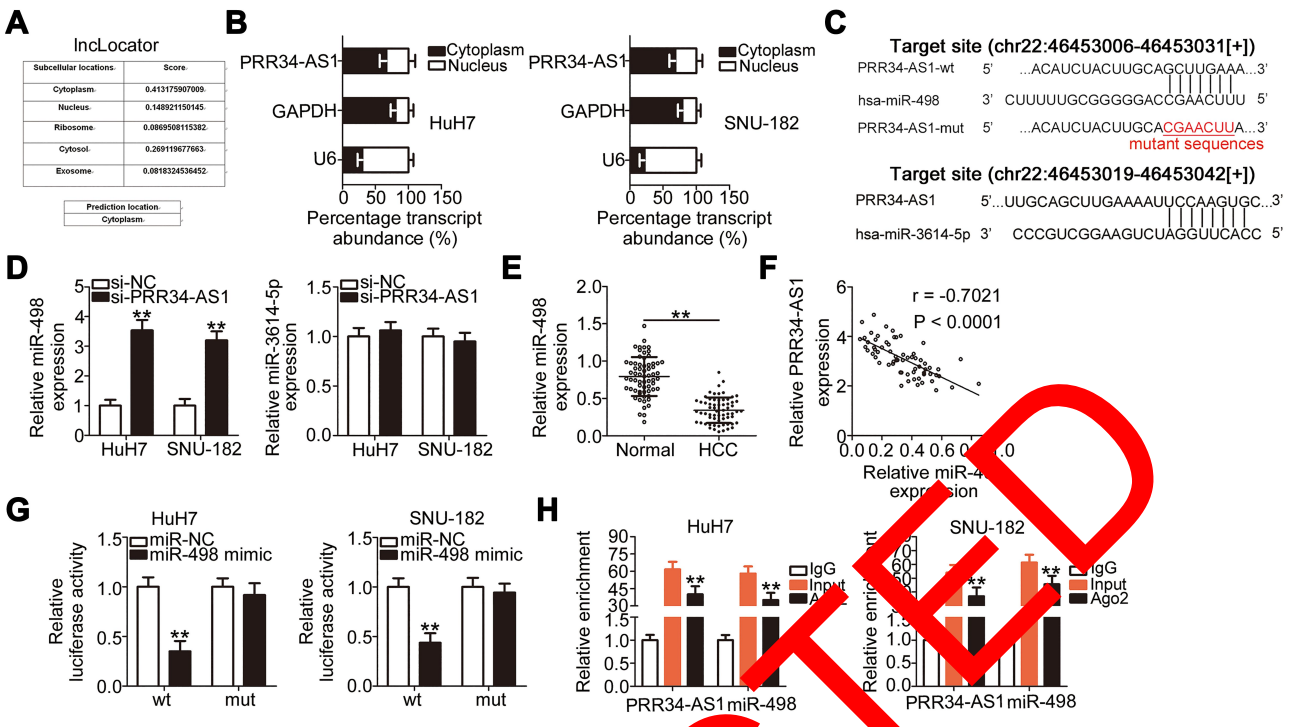

Figure 2 *PRR34-AS1* functions as an miR-498 sponge in HCC cells. (**A**) lncLocator p dicted the subcellular distribution of *PRR34-AS1*. (**B**) Cellular nucleocytoplasmic fractionation was performed to isolate the nuclear and cytoplasmic fractions of HuH and SNU-182 c Both fractions were analyzed via RT-qPCR to determine the localization of *PRR34-AS1* in HCC cells. (**C**) The complementary binding sites of *miR-4* and *miR-3614-5* within *PRR34-AS1*. (**D**) *miR-498* and *miR-3614-5p* expression in PRR34-AS1-depleted HuH7 and SNU-182 cells were measured via RT-qPCR. (**E**) RT-qPC nalysis was us to measure the expression of *miR-498* in 65 pairs of HCC and adjacent normal tissues. (**F**) The correlation between *miR-498* and *PRR34-AS1* levels in 65 HCC ssues was analyzed using Pearson's correlation coefficient. (**G**) Luciferase reporter assays were used to analyze the binding interaction be en *R-498* and *PRR* *S1* in HCC cells. Cotransfection of miR-498 mimic and the wt-PRR34-AS1 reporter plasmid clearly reduced the luciferase activity in HuH7 and SN 182 ce luciferase activity of the mut-PRR34-AS1 reporter plasmid was unchanged after miR-498 mimic cotransfection. (**H**) RIP assay was conducted using the anti-A 2 an ody t termine the enrichment of *miR-498* and *PRR34-AS1* in HuH7 and SNU-182 cells. **P < 0.01.

assays were conducted to analyze he b ding interaction between *miR-498* and *PRR34-A* in HCC ls. The wild-type and mutant binding tes etween *mi 498* and *PRR34-AS1* were pres ed in Figu 2C. As illustrated in Figure 2G, the luc erase activity of th wt-PRR34-AS1 reporter vector bu ot tha of the mut-PRR34-AS1 reporter vector was reduce y *miR-4* upregulation in HuH7 and SNU- 2 ce , indi ins hat *miR-498* directly binds to *PRR -AS1*. F thermore, the RIP assay results demonstrated t *RR34-AS1* and *miR-498* were statistically enriched in a i-Ago2 pellets (Figure 2H). Taken together, these data sugg that *PRR34-AS1* functions as an miR-498 sponge in HCC cells.

miR-498 is an Antioncogenic miRNA in HCC Cells

To identify the roles of *PRR34-AS1* in HCC cells, HuH7 and SNU-182 cells were transfected with miR-498 mimic to generate miR-498-overexpressing cells (Figure 3A). Cell proliferation was detected via the CCK-8 assay, and the results showed that transfection with miR-498 mimic resulted in a substantial decrease in cell proliferation (Figure 3B). Additionally, compared with the miR-NC group, ectopic miR-498 expression strikingly promoted HuH7 and SNU-182 cell apoptosis (Figure 3C). Furthermore, miR-498-overexpressing HuH7 and SNU-182 cells presented impaired migratory (Figure 3D) and invasive (Figure 3E) abilities compared with miR-NC-transfected cells. These results collectively demonstrate that *miR-498* plays cancer-inhibiting roles during HCC progression.

FOXO3 is Directly Targeted by miR-498 Under the Control of PRR34-AS1 in HCC Cells

A previous study has identified *FOXO3* (Figure 4A) as a direct target of *miR-498* in HCC cells. To confirm this observation, wt-FOXO3 and mut-FOXO3 reporter plasmids were constructed and transfected into HuH7 and SNU-182 cells in the presence of miR-498 mimic or miR-NC. The

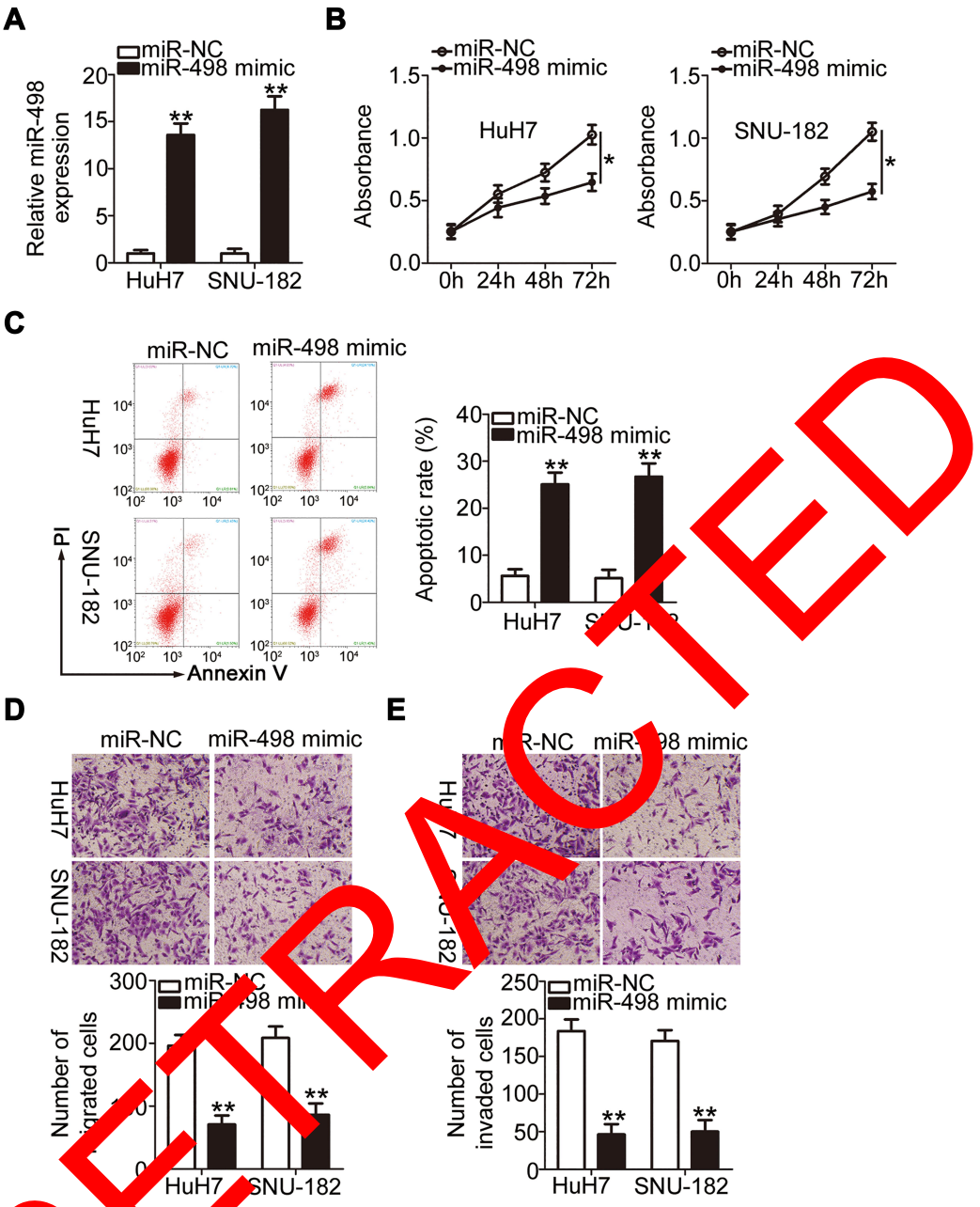

Figure 3 *miR-498* overexpression inhibits the malignant feature of HCC cells. (**A**) The level of *miR-498* was examined via RT-qPCR in miR-498 mimic-transfected or miR-NC -transfected HuH7 and SNU-182 cells. (**B** and **C**) The proliferation and apoptosis of miR-498-overexpressed HuH7 and SNU-182 cells were analyzed via the CCK-8 assay and flow cytometry analysis, respectively. (**D** and **E**) Transwell cell migration and invasion assays were used to examine the migration and invasion of HuH7 and SNU-182 cells after *miR-498* overexpression (x200 magnification). *P < 0.05 and **P < 0.01.

luciferase reporter assay results showed that the luciferase activity of wt-FOXO3 was initially decreased by *miR-498* overexpression, whereas that of mut-FOXO3 was minimally affected in HuH7 and SNU-182 cells (Figure 4B). In addition, transfection with miR-498 mimic led to significantly reduced *FOXO3* expression at both the mRNA (Figure 4C) and protein (Figure 4D) levels in HuH7 and SNU-182 cells. Furthermore, the expression of *FOXO3* mRNA was dramatically upregulated in HCC tissues than in adjacent normal tissues (Figure 4E). Notably, the abundance of *FOXO3* mRNA in the 65 HCC tissue specimens was inversely related to the level of *miR-498* (Figure 4F; $r = -0.6675$, $P < 0.0001$). The above results demonstrate *FOXO3* as a direct target of *miR-498* in HCC cells.

To investigate the manner in which *PRR34-AS1* regulates *FOXO3* levels in HCC cells, the impacts of *PRR34-AS1*

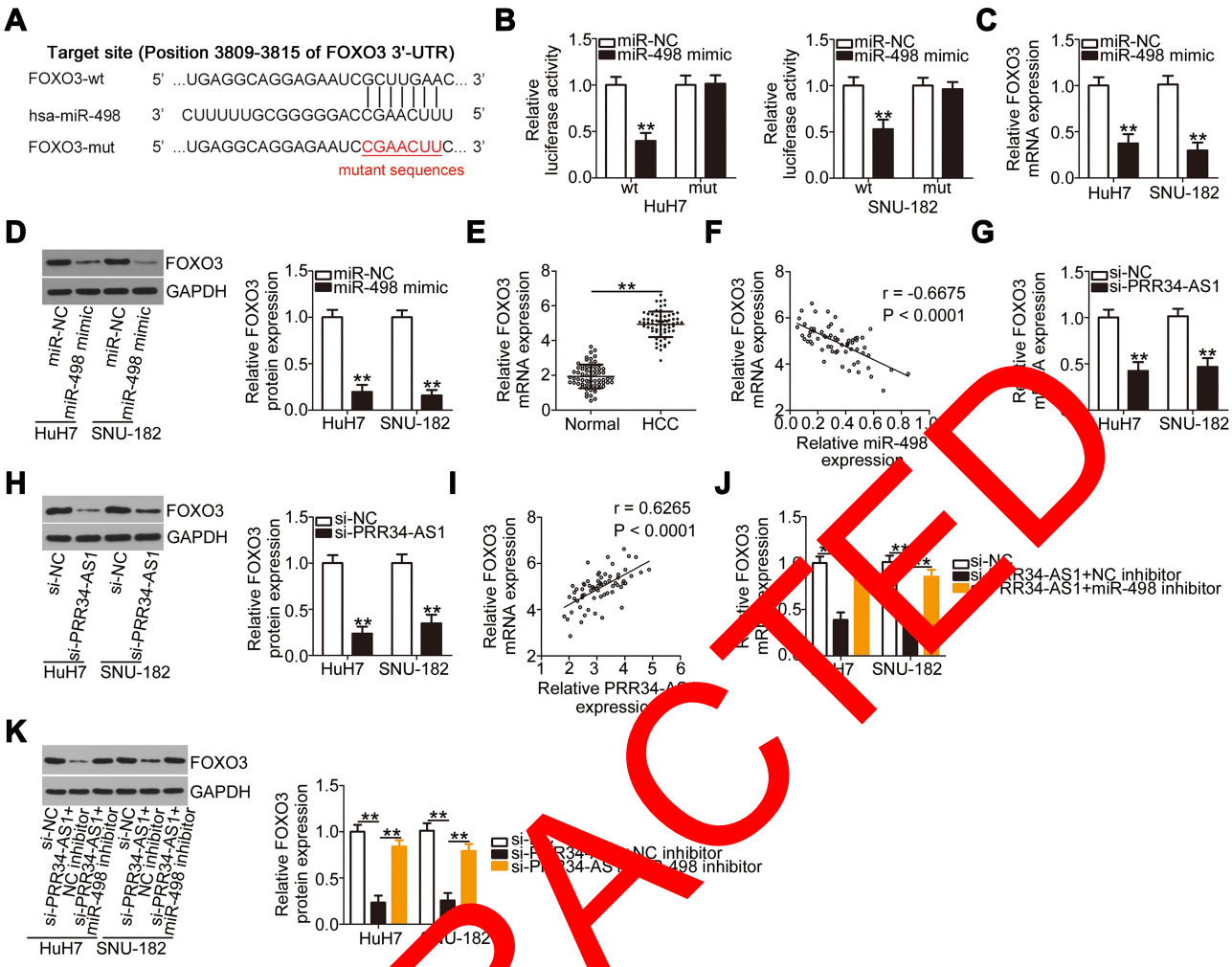

Figure 4 *FOXO3* is directly targeted by *miR-498* in HCC cells and under the regulation of *PRR34-AS1*. (**A**) The complementary binding site between *miR-498* and *FOXO3* was predicted via bioinformatic analysis. (**B**) Luciferase reporter assays were performed in HuH7 and SNU-182 cells cotransfected with miR-498 mimic or miR-NC and wt-FOXO3 or mut-FOXO3. (**C** and **D**) The mRNA and protein expression levels of *FOXO3* were detected in HuH7 and SNU-182 cells after *miR-498* upregulation. (**E**) The mRNA level of *FOXO3* in the 65 pairs of HCC and adjacent normal tissues was tested via RT-qPCR. (**F**) Pearson's correlation coefficient analysis illustrated the correlation between *miR-498* and *FOXO3* mRNA expression in the 65 HCC tissues. (**G** and **H**) The regulatory effects of *PRR34-AS1* deficiency on *FOXO3* mRNA and protein levels in HuH7 and SNU-182 cells were determined via RT-qPCR and Western blotting. (**I**) The relationship between *PRR34-AS1* and *FOXO3* mRNA expression in the 65 HCC tissues was tested using Pearson's correlation coefficient. (**J** and **K**) HuH7 and SNU-182 cells were transfected with miR-498 inhibitor or NC inhibitor in the presence of si-PRR34-AS1, and changes in the expression of *FOXO3* mRNA and protein were examined via RT-qPCR and Western blotting, respectively. **P < 0.01.

silencing of *FOXO3* mRNA and protein expression in HuH7 and SNU-182 cells were evaluated. The results showed that *FOXO3* mRNA (Figure 4G) and protein (Figure 4H) levels were apparently decreased by *PRR34-AS1* depletion. Additionally, *PRR34-AS1* expression presented a positive correlation with *FOXO3* mRNA in the 65 HCC tissues (Figure 4I; r = 0.6265, P < 0.0001). To determine whether *PRR34-AS1* regulates *FOXO3* expression by adsorbing *miR-498*, miR-498 inhibitor or NC inhibitor was transfected into PRR34-AS1-depleted HuH7 and SNU-182 cells. RT-qPCR and Western blotting were used to determine the expression of *FOXO3*. The results confirmed that loss of *PRR34-AS1* obviously decreased *FOXO3* mRNA (Figure 4J) and protein (Figure 4K) expressions in HuH7 and SNU-182 cells. Significantly, this influence was abolished by the addition of the miR-498 inhibitor. Collectively, these results demonstrate that *PRR34-AS1* acts as a molecular sponge for *miR-498* in HCC cells, thereby increasing the expression of its downstream target gene *FOXO3*.

miR-498 Downregulation and FOXO3 Upregulation Both Abrogate the Inhibitory Actions of PRR34-AS1 Downregulation in HCC Cells

To determine whether the biological activities of *PRR34-AS1* in HCC cells are mediated by the regulation of the

miR-498/*FOXO3* axis, HuH7 and SNU-182 cells previously transfected with si-PRR34-AS1 were treated with miR-498 inhibitor or NC inhibitor. The RT-qPCR results verified the transfection efficiency of the miR-498 inhibitor (Figure 5A). si-PRR34-AS1 transfection obviously suppressed HuH7 and SNU-182 cell proliferation (Figure 5B) but promoted their apoptosis (Figure 5C); the effects were alleviated by miR-498 inhibitor treatment. Additionally, the migration (Figure 5D) and invasion (Figure 5E) of HuH7 and SNU-182 cells impaired by PRR34-AS1 deficiency were partially restored by the addition of the miR-498 inhibitor.

Rescue experiments were performed in HuH7 and SNU-182 cells to test whether *FOXO3* was required for the PRR34-AS1-mediated regulation of the malignant features in HCC. First, the overexpression efficiency of pcDNA3.1/FOXO3 was evaluated by measuring the changes in *FOXO3* protein expression in HuH7 and SNU-182 cells after the transfection of pcDNA3.1/FOXO3 or pcDNA3.1. The protein level of *FOXO3* was significantly increased in pcDNA3.1/FOXO3-transfected HuH7 and SNU-182 cells (Figure 5F). pcDNA3.1/FOXO3 or pcDNA3.1, in combination with si-PRR34-AS1, was transfected into HuH7 and SNU-182 cells, and cell proliferation, apoptosis, migration, and invasion were analyzed. Restoring *FOXO3* expression partly reversed the impacts of *PRR34-AS1* silencing on the proliferation (Figure 5G), apoptosis (Figure 5H), migration (Figure 5I), and invasion (Figure 5J) of HuH7 and SNU-182 cells. Therefore, the actions of *PRR34-AS1* in HCC cells were performed by regulating the output of the miR-498/FOXO3 axis.

Loss of PRR34-AS1 Decreases Tumor Growth in HCC Cells in vivo

To address the hepatocarcinogenesis role of *PRR34-AS1* in vivo, xenograft models were established by injecting HuH7 cells stably expressing sh-PRR34-AS1 or sh-NC into nude mice. Tumor volumes (Figure 6A and B) and weights (Figure 6C) were markedly decreased in the subcutaneous tumor xenografts derived from sh-PRR34-AS1 stably transfected HuH7 cells. Tumor xenografts were harvested and subjected to RT-qPCR analysis to determine the expression levels of *PRR34-AS1* and *miR-498*. The data revealed that *PRR34-AS1* was downregulated in the subcutaneous tumors from the sh-PRR34-AS1 group (Figure 6D), whereas the levels of *miR-498* presented the opposite trend (Figure 6E). Additionally, Western blotting analysis revealed that *FOXO3* protein expression was remarkably decreased in PRR34-AS1-deficient tumor xenografts (Figure 6F). Therefore, the interference of *PRR34-AS1*inhibits the tumor growth of HCC due to altered miR-498/FOXO3 expression.

Discussion

Recent studies have discovered that lncRNAs are differentially expressed in HCC, and they have been validated as crucial regulators in HCC cells.[16,29,30] lncRNAs perform important roles in tumor differentiation, growth, metastasis, epithelial–mesenchymal transition, and radiochemotherapy resistance as well as other aspects by regulating gene expression and cancer-related signaling pathways.[31] Therefore, further studies on tumor-associated lncRNAs in HCC are warranted for the identification of potential therapeutic targets. In the current study, the expression and detailed roles of *PRR34-AS1* in HCC were determined. In addition, a series of mechanistic studies were performed to elucidate the interactions of *PRR34-AS1* with miRNAs and mRNAs in relation to its regulation of HCC oncogenicity.

PRR34-AS1 has been shown to promote the protection of dexmedetomidol pretreatment against ischemia/reperfusion injury;[32] however, the expression and functions of *PRR34-AS1* in HCC cells remain poorly understood. In the present study, TCGA and GTEx databases and clinical specimens were used to evaluate the expression of *PRR34-AS1* in HCC cells. The expression of *PRR34-AS1* in HCC tissues was higher than that in normal tissues. Following *PRR34-AS1*silencing in vitro, we assessed the changes in HCC cell proliferation, apoptosis, migration, and invasion. Our results displayed that *PRR34-AS1* interference inhibited HCC cell proliferation, migration, and invasion and promoted cell apoptosis. Tumor xenograft experiments confirmed that loss of *PRR34-AS1* reduced tumor growth in HCC cells in vivo.

The above findings led us to investigate the precise mechanisms by which *PRR34-AS1* regulates the aggressiveness of HCC cells. The ceRNA regulation theory has recently been proposed to describe the working mechanism of cytoplasmic lncRNAs.[33] lncRNAs harbor miRNA-response elements and can compete with other genes to bind to miRNAs, thereby decreasing the miRNA-mediated suppression of miRNA targets.[26] Accordingly, the localization of *PRR34-AS1* was first predicted using lncLocator, a lncRNA subcellular localization predictor. In addition,

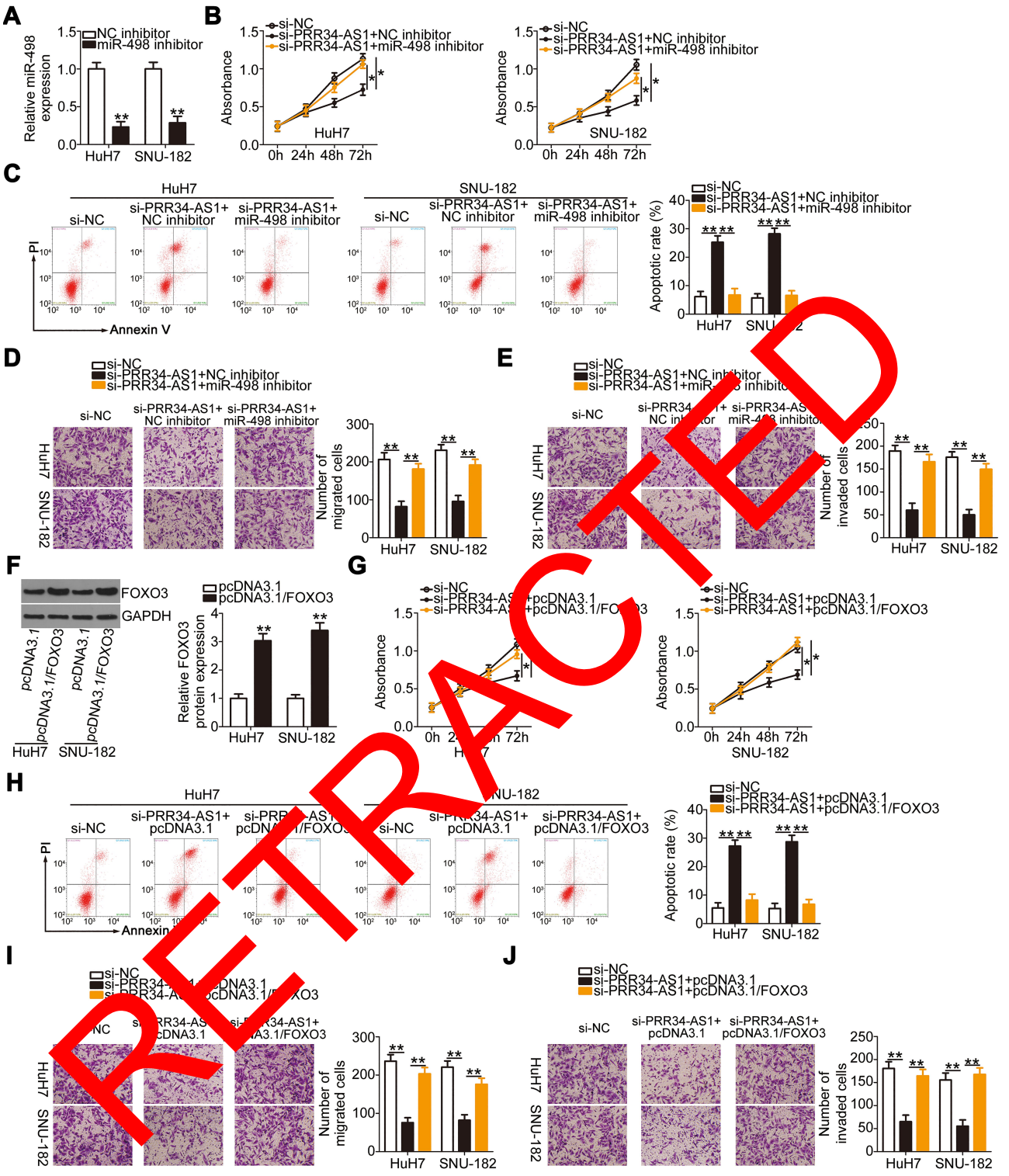

Figure 5 The effects of *PRR34-AS1* downregulation on the malignant features of HCC cells are mediated by the miR-498/FOXO3 axis. (**A**) RT-qPCR was performed to detect the expression of *miR-498* in HuH7 and SNU-182 cells after miR-498 inhibitor or NC inhibitor injection. (**B**–**E**) miR-498 inhibitor or NC inhibitor, alongside si-PRR34 -AS1, was transfected into HuH7 and SNU-182 cells. Proliferation, apoptosis, migration, and invasion were examined via the CCK-8 assay, flow cytometric analysis, and transwell cell migration and invasion assays (x200 magnification), respectively. (**F**) Western blotting assessed the efficiency of pcDNA3.1/FOXO3 treatment in HuH7 and SNU-182 cells. (**G**–**J**) CCK-8 assay, flow cytometric analysis, and transwell cell migration and invasion assays (x200 magnification) were used to investigate the proliferation, apoptosis, migration, and invasion, respectively, of HuH7 and SNU-182 cells after cotransfection with pcDNA3.1/FOXO3 or pcDNA3.1 and si-PRR34-AS1. *P < 0.05 and **P < 0.01.

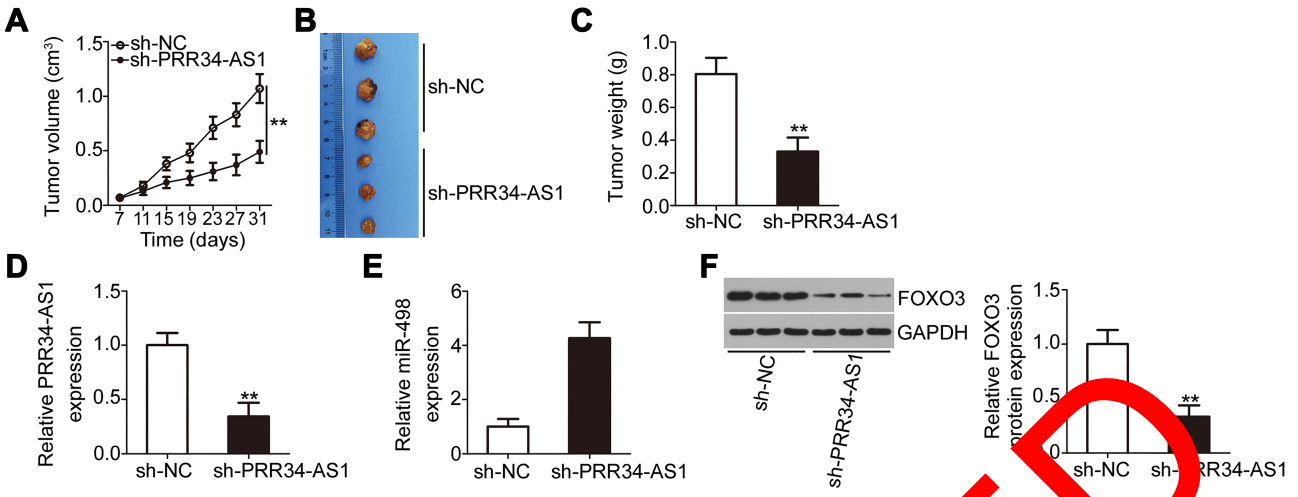

Figure 6 Interference of *PRR34-AS1* reduces HCC tumor growth in vivo. (**A**) HuH7 cells stably expressing sh-PRR34-AS1 or sh-NC were subcutaneously injected into nude mice. Tumor volume was detected every 4 days. (**B**) All mice were euthanized at the end of the experiment, and the tumor xenografts were harvested and imaged. (**C**) Tumor weight was measured on day 31 after cell injection. (**D** and **E**) *PRR34-AS1* and *miR-498* expression in the tumor xenografts were detected via RT-qPCR. (**F**) Western blotting was used to examine the protein level of *FOXO3* in tumor xenografts obtained from sh-PRR34-AS1 and sh-NC groups. **P < 0.01.

cellular nucleocytoplasmic fractionation was performed to isolate the nuclear and cytoplasmic fractions of HCC cells. Both fractions were subjected to RT-qPCR analysis to determine the distribution of *PRR34-AS1*. *PRR34-AS1* was found to be mostly distributed in the cytoplasm of HCC cells, implying its potential ability to function as a molecular sponge for miRNAs.

Using bioinformatics analysis, *miR-498* and *miR-3614-5p* were predicted to be sequestered by *PRR34-AS1*.*miR-498* and *miR-3614-5p* expression was also restored *PRR34-AS1* silencing in HCC cells were determined using RT-qPCR. *miR-498* was identified as the only one candidate whose expression was strikingly increased in HCC cells after *PRR34-AS1* depletion. Moreover, *miR-498* was downregulated in HCC tissues, and an inverse correlation was identified between the expression levels of *miR-498* and *PRR34-AS1* in HCC tissues. Furthermore, luciferase activity and RIP assays verified the direct binding relationship between *miR-498* and *PRR34-AS1* in HCC cells. After validating *FOXO3* as a direct target of *miR-498*, we further explored the regulatory relationship among *PRR34-AS1*, *miR-498*, and *FOXO3* in HCC cells. Our results demonstrated that *PRR34-AS1* positively regulates *FOXO3* expression in HCC cells by acting as an *miR-498* sponge. Taken together, a ceRNA regulatory network involving *PRR34-AS1*, *miR-498*, and *FOXO3* was identified in HCC cells.

miR-498 is expressed at low levels in many types of human cancers, including HCC.[34] The results of functional experiments illustrate the tumor-suppressing functions of *miR-498* in HCC cells, which are consistent with those of a previous study.[34] *FOXO3*, a direct target of *miR-498* in HCC cells, is a member of the forkhead box class O transcription factor family.[35] Studies have revealed the high expression of *FOXO3* in HCC cells and have confirmed its pro-oncogenic actions during HCC genesis and progression.[36–38] In the present study, rescue experiments were conducted, and the results showed that the suppressive effects triggered by *PRR34-AS1* knockdown on the malignant features of HCC cells could be abrogated by inhibiting *miR-498* or restoring *FOXO3*. Taken together, it can be inferred that *PRR34-AS1* acts as an *miR-498* sponge to increase the expression of *FOXO3* in HCC cells, thereby exhibiting cancer-promoting actions during cancer progression.

In this study, we did not overexpress *PRR34-AS1* expression, and determine the effects of *PRR34-AS1* upregulation on the malignant phenotypes of HCC cells. Additionally, we did not explore whether knockdown of *PRR34-AS1* may regulate important signal pathways in HCC. They were limitations of our study, and we will resolve them in the near future.

Conclusion

In summary, *PRR34-AS1* is significantly highly expressed in HCC tissues and cell lines. *PRR34-AS1* promotes the oncogenicity of HCC cells by adsorbing *miR-498* and subsequently increasing the expression of *FOXO3*.

Therefore, the PRR34-AS1/miR-498/FOXO3 pathway may offer a basis for HCC treatment.

Disclosure

The authors declare that they have no competing interests.

References

1. Siegel RL, Miller KD, Jemal A. Cancer statistics, 2019. *CA Cancer J Clin*. 2019;69(1):7–34.
2. Hartke J, Johnson M, Ghabril M. The diagnosis and treatment of hepatocellular carcinoma. *Semin Diagn Pathol*. 2017;34(2):153–159. doi:10.1053/j.semdp.2016.12.011
3. Siegel RL, Miller KD, Jemal A. Cancer statistics, 2017. *CA Cancer J Clin*. 2017;67(1):7–30.
4. Kulik L, El-Serag HB. Epidemiology and management of hepatocellular carcinoma. *Gastroenterology*. 2019;156(2):477–491 e471. doi:10.1053/j.gastro.2018.08.065
5. Portolani N, Coniglio A, Ghidoni S, et al. Early and late recurrence after liver resection for hepatocellular carcinoma: prognostic and therapeutic implications. *Ann Surg*. 2006;243(2):229–235. doi:10.1097/01.sla.0000197706.21803.a1
6. Ye LY, Chen W, Bai XL, et al. Hypoxia-induced epithelial-to-mesenchymal transition in hepatocellular carcinoma induces an immunosuppressive tumor microenvironment to promote metastasis. *Cancer Res*. 2016;76(4):818–830. doi:10.1158/0008-5472.CAN-15-0977
7. Forner A, Reig M, Bruix J. Hepatocellular carcinoma. *Lancet*. 2018;391(10127):1301–1314. doi:10.1016/S0140-6736(18)30010-2
8. Said A, Ghufran A. Epidemic of non-alcoholic fatty liver disease and hepatocellular carcinoma. *World J Clin Oncol*. 2017;8(6):42[illegible]436. doi:10.5306/wjco.v8.i6.429
9. St Laurent G, Wahlestedt C, Kapranov P. The [illegible]pe of long noncoding RNA classification. *Trends Genet*. 2015;31[illegible]:239–25[illegible] doi:10.1016/j.tig.2015.03.007
10. Melissari MT, Grote P. Roles for long non-coding RNAs in physiology and disease. *Pflugers Arch*. 201[illegible]468(6):9[illegible]58. doi:10.1007/s00424-016-1804-y
11. Huarte M. The emerging role of lncRNAs in cancer. *Nat Med*. 2015;21(11):1253–1261.
12. Liz J, Esteller M. lncRNAs and microRNAs with a role in cancer development. *Biochim Biophys Acta*. 2016;1859(1):169–176. doi:10.1016/j.bbagrm.2015.06.015
13. Wu Y, Shao A, Wang L, et al. The role of lncRNAs in the distant metastasis of breast cancer. *Front Oncol*. 2019;9:407. doi:10.3389/fonc.2019.00407
14. Hu P, Miao Y, Yu S, Gu N. Long non-coding RNA SNHG5 promotes human hepatocellular carcinoma progression by regulating miR-363-3p/CDC42EP3/BAF38 axis. *Eur Rev Med Pharmacol Sci*. 2020;24(7):3592–3[illegible]
15. Shi C, Yang [illegible], Pan S, et al. LncRNA OIP5-AS1 promotes cell proliferation and migration and induces angiogenesis via regulating miR-3163/VEGFA in hepatocellular carcinoma. *Cancer Biol Ther*. 2020;21:604–614. doi:10.1080/15384047.2020.1738908
16. Wang C, Zi H, Wang Y, Li B, Ge Z, Ren X. LncRNA CASC15 promotes tumour progression through SOX4/Wnt/beta-catenin signalling pathway in hepatocellular carcinoma. *Artif Cells Nanomed Biotechnol*. 2020;48(1):763–769. doi:10.1080/21691401.2019.1576713
17. Shao C, Liu G, Zhang X, Li A, Guo X. Long noncoding RNA RMRP suppresses the tumorigenesis of hepatocellular carcinoma through targeting microRNA-766. *Onco Targets Ther*. 2020;13:3013–3024. doi:10.2147/OTT.S243736
18. Bi HQ, Li ZH, Zhang H. Long noncoding RNA HAND2-AS1 reduced the viability of hepatocellular carcinoma via targeting microRNA-300/SOCS5 axis. *Hepatobiliary Pancreat Dis Int*. 2020. doi:10.1016/j.hbpd.2020.02.011
19. Gao L, Xiong DD, He RQ, et al. MIR22HG as a tumor suppressive lncRNA in HCC: a comprehensive analysis integrating RT-qPCR, mRNA-seq, and microarrays. *Onco Targets Ther*. 2019;12:9827–9848. doi:10.2147/OTT.S227541
20. Liu WG, Xu Q. Long non-coding RNA XIST promotes hepatocellular carcinoma progression by sponging miR-200b-3p. *Eur Rev Med Pharmacol Sci*. 2019;23(22):9857–9862.
21. Tian X, Wu Y, Yang Y, et al. Long noncoding RNA LINC00662 promotes M2 macrophage polarization and hepatocellular carcinoma progression via activating Wnt/β-catenin signaling. *Mol Oncol*. 2020;14(2):462–483. doi:10.1002/1878[illegible]12606
22. Harries LW. Long non-coding RNAs and human disease. *Biochem Soc Trans*. 2012;40(4):902–906. doi:10.1042/BST[illegible]0120020
23. Lajos R, Braicu C, Jurj A, et al. A[illegible]iRNAs profile evolution of triple negative breast cancer cells in the presence of a possible adjuvant therapy and senescence inducer. *J BUON*. 2018;23(3):692–705.
24. Rui T, Xu S, Feng [illegible], Zhang X, Huang H, [illegible]g Q. The mir-767-105 cluster: a crucial factor related to the poor prognosis of hepatocellular carcinoma. *Biomark Res*. 2020;8:7. doi:10.1186/s40364-020-0186-7
25. Yu D, Zh[illegible] Tu H, Wu [illegible], Yang [illegible], Xu C. miR-4698-Trim59 axis plays a suppressive role in hepatocellular carcinoma. *Front Biosci*. 2020;25:1120–1[illegible] doi:10.2741/4849
26. Ab[illegible]allahzadeh R, [illegible]aei A, Mansoori Y, Sepahvand M, Amoli MM, Tavakkoly-Bazzaz J. Competing endogenous RNA (ceRNA) cross talk and language in ceRNA regulatory networks: a new look at hallmarks of breast cancer. *J Cell Physiol*. 2019;234(7):10080–1[illegible]00. doi:10.1002/jcp.27941
27. [illegible]in Y, Ji[illegible]Z, Jin H, et al. Long non-coding RNA DLGAP1-AS1 facilitates tumorigenesis and epithelial-mesenchymal transition in hepatocellular carcinoma via the feedback loop of miR-26a/b-5p/IL-6/JAK2/STAT3 and Wnt/beta-catenin pathway. *Cell Death Dis*. 2020;11(1):34. doi:10.1038/s41419-019-2188-7
28. Wu S, Chen S, Lin N, Yang J. Long non-coding RNA SUMO1P3 promotes hepatocellular carcinoma progression through activating Wnt/beta-catenin signalling pathway by targeting miR-320a. *J Cell Mol Med*. 2020;24(5):3108–3116. doi:10.1111/jcmm.14977
29. Gong X, Zhu Z. Long noncoding RNA HOTAIR contributes to progression in hepatocellular carcinoma by sponging miR-217-5p. *Cancer Biother Radiopharm*. 2020. doi:10.1089/cbr.2019.3070
30. Fan L, Huang X, Chen J, et al. Long non-coding RNA MALAT1 contributes to sorafenib resistance by targeting miR-140-5p/Aurora-A signaling in hepatocellular carcinoma. *Mol Cancer Ther*. 2020;19:1197–1209. doi:10.1158/1535-7163.MCT-19-0203
31. Huang Z, Zhou JK, Peng Y, He W, Huang C. The role of long noncoding RNAs in hepatocellular carcinoma. *Mol Cancer*. 2020;19(1):77.
32. Fang H, Zhang FX, Li HF, et al. PRR34-AS1 overexpression promotes protection of propofol pretreatment against ischemia/reperfusion injury in a mouse model after total knee arthroplasty via blockade of the JAK1-dependent JAK-STAT signaling pathway. *J Cell Physiol*. 2020;235(3):2545–2556. doi:10.1002/jcp.29158
33. Ye Y, Shen A, Liu A. Long non-coding RNA H19 and cancer: a competing endogenous RNA. *Bull Cancer*. 2019;106(12):1152–1159. doi:10.1016/j.bulcan.2019.08.011
34. Li W, Jiang H. Up-regulation of miR-498 inhibits cell proliferation, invasion and migration of hepatocellular carcinoma by targeting FOXO3. *Clin Res Hepatol Gastroenterol*. 2020;44(1):29–37. doi:10.1016/j.clinre.2019.04.007
35. Huang H, Tindall DJ. Dynamic FoxO transcription factors. *J Cell Sci*. 2007;120(Pt 15):2479–2487. doi:10.1242/jcs.001222
36. Song SS, Ying JF, Zhang YN, et al. High expression of FOXO3 is associated with poor prognosis in patients with hepatocellular carcinoma. *Oncol Lett*. 2020;19(4):3181–3188.

37. Zhao W, Dai Y, Dai T, et al. TRIP6 promotes cell proliferation in hepatocellular carcinoma via suppression of FOXO3a. *Biochem Biophys Res Commun*. 2017;494(3–4):594–601. doi:10.1016/j.bbrc.2017.10.117

38. Yang Z, Liu S, Zhu M, et al. PS341 inhibits hepatocellular and colorectal cancer cells through the FOXO3/CTNNB1 signaling pathway. *Sci Rep*. 2016;6:22090.